

See discussions, stats, and author profiles for this publication at: <https://www.researchgate.net/publication/281591508>

# Tracing the Compositional Changes of Asphaltenes after Hydroconversion and Thermal Cracking Processes by High-Resolution Mass Spectrometry

ARTICLE *in* ENERGY & FUELS · SEPTEMBER 2015

Impact Factor: 2.79 · DOI: 10.1021/acs.energyfuels.5b01510

---

READS

39

## 5 AUTHORS, INCLUDING:



Marianny Y. Combariza

Industrial University of Santander

31 PUBLICATIONS 361 CITATIONS

[SEE PROFILE](#)



Martha Liliana Chacón

Industrial University of Santander

3 PUBLICATIONS 11 CITATIONS

[SEE PROFILE](#)



Jorge A. Orrego-Ruiz

Instituto Colombiano del Petroleo

16 PUBLICATIONS 47 CITATIONS

[SEE PROFILE](#)



Andrea Gómez-Escudero

Instituto Colombiano del Petroleo

8 PUBLICATIONS 49 CITATIONS

[SEE PROFILE](#)

# Tracing the Compositional Changes of Asphaltenes after Hydroconversion and Thermal Cracking Processes by High-Resolution Mass Spectrometry

Martha L. Chacón-Patiño,<sup>†</sup> Cristian Blanco-Tirado,<sup>†</sup> Jorge A. Orrego-Ruiz,<sup>‡</sup> Andrea Gómez-Escudero,<sup>‡</sup> and Marianny Y. Combariza\*,<sup>†</sup>

<sup>†</sup>Escuela de Química, Universidad Industrial de Santander, Bucaramanga, Santander 680002, Colombia

<sup>‡</sup>ECOPETROL, Instituto Colombiano del Petróleo, Piedecuesta, Santander 681018, Colombia

## Supporting Information

**ABSTRACT:** With heavy crude oil refining on the rise, upgrading strategies are fundamental to yield high-value products. Hydroconversion and thermal cracking are well-established and widely used upgrading processes for heavy oils' distillation cuts and residues. Recognizing molecular changes in these fractions after upgrading, particularly of asphalteneic compounds, is fundamental to understand and optimize the processes. In this work, we follow compositional changes in the asphaltene fraction of a Colombian heavy crude, after hydroconversion and thermal cracking, using high-resolution mass spectrometry. The liquid products from the upgrading processes were fractionated into maltenes and residual asphaltenes, with yields between 33% and 38% in maltenes from the original asphaltene feedstock. Contoured plots of double bond equivalents versus carbon number and van Krevelen diagrams show maltenic fractions exhibiting lower aromaticity, smaller molecular size, fewer heteroatomic species, and higher content of alkyl side chains than the starting asphalteneic material. Residual asphaltenes, on the other hand, consist of compounds with lower H/C ratios and reduced content of alkyl groups than the feedstock. In addition, structural information about the feedstock, such as archipelago or island structures, can be derived from the plots. This information is useful to establish trends between compound class reactivity and the suitability to produce valuable maltenic compounds through upgrading technologies.

## INTRODUCTION

Nowadays, with light crude oil reserves around the globe dramatically depleted, the petrochemical industry's attention is rapidly shifting to nonconventional hydrocarbons, such as heavy and extra-heavy oils and bitumens.<sup>1–3</sup> Refining strategies for these highly complex hydrocarbon mixtures involve a traditional atmospheric or vacuum distillation, followed by upgrading of the residues by catalytic and noncatalytic processes.<sup>1,4</sup> Hydroconversion, which is an example of the former, and thermal cracking, which is a representative of the latter, are well-known as upgrading alternatives widely used for synthetic petroleum production.<sup>5,6</sup> Hydrogenation, deoxidization, denitrogenation, and desulfurization of polynuclear aromatics and heteroaromatic compounds occur simultaneously in hydroconversion processes, while heavy metals such as nickel and vanadium are removed.<sup>7,8</sup> In thermal cracking processes, primary reactions involve thermolysis of aromatic–alkyl bonds, to produce light hydrocarbons, whereas secondary reactions, such as dehydrogenation of naphthenic moieties and condensation of aromatic units, produce coke precursors.<sup>9,10</sup>

Macroscopic properties such as API grade, SARA composition, and elemental analysis are not enough to predict ideal operational conditions in upgrading processes, particularly for nonconventional hydrocarbons.<sup>11</sup> For this reason, tracking compositional changes in heavy oils before and after the upgrading processes is of fundamental importance to design tailored refining strategies aimed to increase yields of valued products. However, not every fraction of the heavy oil has an

"unpredictable" behavior upon upgrading.<sup>12</sup> Among the saturated, aromatic, resin, and asphaltene fractions present in a crude oil, the latter has become increasingly abundant and is considered the most problematic during upstream and downstream stages.<sup>13</sup>

Defined by solubility, asphaltenes are the crude oil fraction insoluble in *n*-heptane and soluble in aromatic solvents such as toluene or benzene.<sup>14</sup> These complex mixtures have molecular structures consisting mostly of pericondensed aromatic rings with heteroatoms (N, O, and S) present in the form of functional groups such as thiophene, sulfide, sulfoxide, hydroxyl, carbonyl, carboxyl, pyrrol, and pyridine, among others.<sup>15–17</sup> The asphalteneic fraction of a crude is also associated with high concentrations of heavy metals such as V and Ni, which are commonly found in the form of metal complexes as petro-porphyrins.<sup>18,19</sup> These molecular features promote the self-aggregation of asphaltenes, which is a behavior restricting comprehensive structural characterization of these molecules.<sup>20–22</sup> Recently, a supramolecular model for asphaltene aggregation have been proposed by Gray et al.,<sup>23</sup> in which intermolecular forces such as hydrogen bonding, acid–base interactions, metal coordination, and  $\pi$ – $\pi$  stacking play a role in producing highly stable asphaltene aggregates. Generally speaking, asphaltene aggregation causes damage in crude oil

Received: July 2, 2015

Revised: September 4, 2015

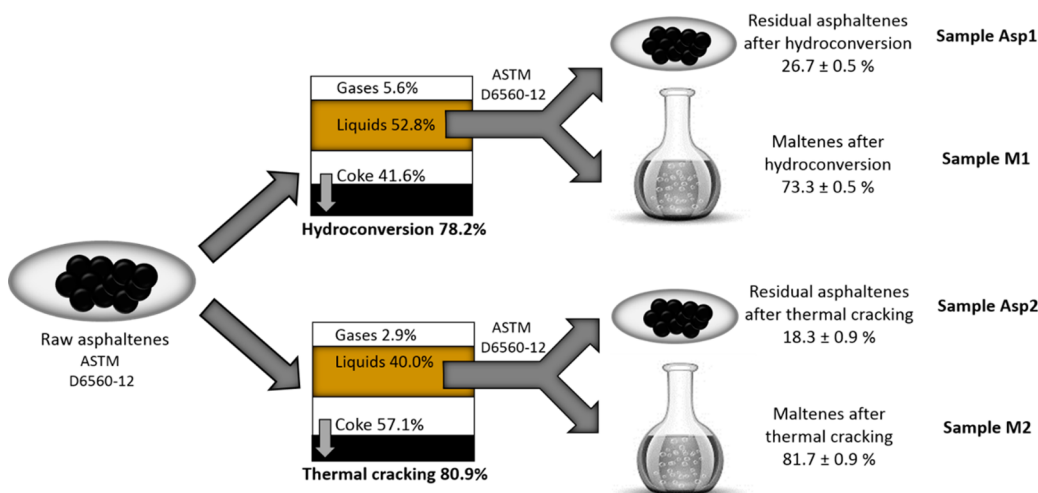


**Figure 1.** Sample evolution and mass balances for a Colombian asphaltene exposed to hydroconversion and thermal cracking upgrading process.

reservoirs, pipeline deposits in transport systems, and difficult situations in the refinery.<sup>24</sup> Also, because of their high heavy metal and sulfur contents, and their high potential to produce coke, asphaltenes are known as the “bad guys” in upgrading processes, particularly of catalytic and thermal nature.<sup>25,26</sup>

Several analytical approaches, involving nuclear magnetic resonance (NMR), X-ray diffraction (XRD), and infrared spectroscopy (IR), have been used to follow the molecular modification of asphaltenes upon upgrading. For example, Ancheyta et al.,<sup>27</sup> who used NMR to study molecular changes in Maya asphaltenes after hydrotreatment, reported the production of lighter asphaltenes with reduced sulfur content and increased aromaticity. Along the same lines, Merdrignac et al.<sup>28</sup> found that structural evolution during hydroconversion is marked by a decrease in asphaltene size and an increase in aromaticity, as a result of molecular dealkylation. On the other hand, Liu et al.,<sup>29</sup> by combining XRD, NMR, and IR, determined that hydrocracking causes a decrease in aromatic and alkyl carbon content in Venezuelan asphaltenes, while the amount of naphthenic carbon increases. Although these approaches provide useful chemical information, a detailed compositional picture of asphaltene evolution is still not available.

Recently, atmospheric pressure photoionization coupled with high-resolution Fourier transform ion cyclotron mass spectrometry (APPI FT-ICR-MS) has emerged as a robust and reliable technique for molecular characterization of complex mixtures such as asphaltenes and vacuum residues.<sup>31,32</sup> In this regard, McKenna et al.,<sup>31</sup> using APPI FT-ICR-MS to study asphaltene’s molecular composition, were able to resolve more than 30 000 ion signals in a single sample, defining the asphaltene compositional space. Unlike spectroscopic techniques, which reflect average properties such as aromaticity or alkyl side-chain content, high-resolution mass spectrometry provides a detailed view of each accessible compound in a complex sample. Only the high resolving power and the mass accuracy offered by FT-ICR MS allows the assignment of elemental compositions to detected ions in mixtures having up to 50 000 different chemical species.<sup>33</sup> To the best of our knowledge, there is only one report dealing with the use of ultrahigh-resolution mass spectrometry for the thorough analysis of asphaltene’s compositional changes after upgrading. Purcell et al.,<sup>11</sup> used APPI FT-ICR MS to follow the

transformation of Iraqi asphaltenes after hydroconversion. The authors found not only that the upgrading process increases asphaltene aromaticity, as has been reported by using other analytical techniques, but also that compound classes of the S<sub>x</sub> type are transformed to S<sub>x-1</sub> classes in the products.

Use of high-resolution mass spectrometry to track upgrading processes is beneficial from many points of view, since it could be used to tune the upgrading process and observe the effects of operational conditions on the molecular features of the products. Besides, in the case of heavy fractions, the technique could also provide some insights into the molecular architecture of difficult compounds such as asphaltenes. On this subject, Gray et al.,<sup>30</sup> through analysis of the distillable fraction from the hydrocracking products using gas chromatography field ionization time-of-flight high-resolution mass spectrometry (GC-FD-TOF HR-MS), suggested the presence of basic building blocks, such as 1–4 ring naphthenes, 1–3 ring aromatics, mono- and dibenzothiophenes, among others, in asphaltenes from different geological origins.

In this contribution, we subjected the asphaltene fraction, from a heavy Colombian crude oil, to hydroconversion and thermal cracking processes and used APPI FT-ICR mass spectrometry to track compositional changes in the products after the upgrading. Liquid products from the thermal process and hydroconversion were fractionated into asphaltenes and maltenes, following the procedure described by ASTM Standard D6560-12, and were further analyzed by APPI FT-ICR MS. We found that the asphaltene feedstock undergo the same chemical transformations with hydroconversion and thermal cracking. For example, the maltenic fraction originated from both processes exhibits lower molecular-weight distributions, higher H/C ratios, high degree of alkyl substitution, and lower heteroatom content than the starting material. The residual asphaltenes exhibit also lower molecular-weight distributions and lower H/C ratios and degree of alkyl substitution than the original asphaltenes. In addition, a retrospective analysis of the upgrading products, particularly the remaining asphaltenes, gave us some insights into the molecular architecture of the parent asphaltenes. In this context, we believe that a detailed description of asphaltene’s transformation could guide efficient upgrading strategies that will eventually impact the economic value of heavy crude oils positively.

## ■ EXPERIMENTAL SECTION

**Sample Preparation.** Colombian asphaltenes were extracted from a heavy crude (API = 12), following the methodology described by ASTM Standard D6560-12.<sup>34</sup> Briefly, 1 g of crude oil was mixed with 40 mL of *n*-C<sub>7</sub> and heated for 40 min under reflux. The mixture was stored in darkness overnight and the precipitated raw asphaltenes were collected by filtration. Asphaltene cleaning was performed recycling *n*-C<sub>7</sub>, in a Soxhlet apparatus, until the solvent was clear. Finally, the clean asphaltenes were recovered by dissolution of the remaining solid in hot toluene, which was subsequently rotoevaporated to produce a clean sample. The raw asphaltene sample was subjected to hydroconversion and thermal cracking processes in a batch microreactor that was equipped with a fluidized sand bath, under the following conditions: for the thermal cracking process, 4 g of asphaltenes were heated during 20 min at 430 °C under a nitrogen atmosphere at a pressure of 0.69 MPa. For the hydroconversion process, 4 g of the asphaltene sample were mixed with 100 ppm of molybdenum naphthenate and reacted for 1 h at 430 °C and 13.7 MPa under hydrogen atmosphere. After the reactions, the liquid products were separated and kept for mass spectrometric analysis.

**Elemental Analysis.** Elemental analysis (CHNS) of the raw asphaltenes and the liquid products from hydroconversion and thermal cracking processes were carried out in a FLASH 2000 analyzer (Thermo Scientific, Billerica, MA, USA). The samples (2–3 mg) were catalytically combusted at 1200 °C.

**Sample Preparation.** The liquid products from the hydroconversion and the thermal cracking processes were also subjected to the ASTM Standard D6560-12 method with the purpose of obtaining the maltenic and the residual asphaltenic fractions. In this fashion, five samples were obtained for mass spectrometric analysis: raw asphaltenes, residual asphaltenes and maltenes from hydroconversion (Asp1 and M1, respectively), and residual asphaltenes and maltenes from thermal cracking (Asp2 and M2, respectively). Figure 1 shows sample evolution and mass balances for each upgrading process. For FT-ICR MS analysis of the raw asphaltenes and their upgrading products, the samples were diluted in toluene to a concentration below 0.30 mg/mL.

**APPI (+) FT-ICR Mass Spectrometry.** Mass spectrometric analysis was performed on a FT-ICR mass spectrometer (SolariX 15 T, Bruker Daltonics, Billerica, MA) equipped with an APPI source, operated in positive (+) mode, fitted with a Krypton photoionization lamp (10.6 eV). Each spectrum was recorded by the accumulation of 100 scans of time-domain transient signals in four mega-point time-domain datasets. The front and back trapping voltages in the ion cyclotron cell were set at +0.70 V and +0.50 V, respectively. The ICR cell was calibrated using a NaTFA solution (*m/z* from 200 to 1200). All mass spectra were internally recalibrated using a homologous series of alkylated compounds. Section S-II in the Supporting Information presents the recalibration output for each spectrum. A resolving power higher than 550 000 at *m/z* 400, for all mass spectra, and a mass accuracy below 1.0 ppm provided unambiguous molecular formula assignments for singly charged ions, either as radical cations M•<sup>+</sup> or protonated molecules [M+H]<sup>+</sup>, with a relative abundance above 0.5%. Mass spectra were processed using the Composer software 1.0.6 (Sierra Analytics, Modesto, CA, USA). Detailed APPI source conditions and other instrumental parameters, as well as

molecular assignment performance, are provided in sections S-I and S-II in the Supporting Information, respectively.

## ■ RESULTS AND DISCUSSION

Hydroconversion and thermal cracking are well-studied and widely used as upgrading technologies. In addition, because of their high potential to produce high-quality valuable products from heavy fractions, they are also attractive for the molecular modification of asphaltenes.<sup>25,26,30</sup> Figure 1 includes mass balances for the upgrading processes, as well as catalytic hydroconversion and thermal conversion percentages. At first glance, it seems that the asphaltene feedstock behaves similarly in both processes, particularly in terms of liquid and coke yields. However, fractionation of the liquids according to the procedure described by ASTM Standard D6560-12 results in different amounts of residual asphaltenes and produced maltenes. In the case of hydroconversion, 73.3% of the liquids are maltenes, according to the *n*-C<sub>7</sub> solubility definition, while after thermal cracking maltenes correspond to 81.7% of the liquid products (Figure 1). Thus, the net yield of maltenes in hydroconversion and thermal cracking were ~38% and ~33%, respectively. Our results indicate that both processes have the potential to produce valuable products from Colombian asphaltenes, with hydroconversion yielding more useful products. On this subject, Savage et al.<sup>35</sup> have reported maltenes yields between 20% and 35% from hydrocracking of North American asphaltenes, and found that the percentage of residual asphaltenes increases from 30% to 45% as the temperature increases from 350 °C to 450 °C. In this study, the liquid products from thermal cracking and hydroconversion, contain ~18% and ~27% of *n*-C<sub>7</sub> of insoluble material or residual asphaltenes, respectively.

We found 48.4% and 51.9% of coke yield for hydroconversion and thermal cracking, respectively, in accordance with the literature. For example, Karimi et al.<sup>36</sup> observed a conversion of ~50% of an asphaltene feedstock to coke under thermal cracking conditions. In another work, Gray et al.<sup>30</sup> reported minimal coke production (~10%) from hydrocracking asphaltenes when using a hydrogen-donor solvent and an iron-based catalyst.

Elemental composition of raw asphaltenes and the liquid products from each upgrading process are shown in Table 1. Conversion is characterized by an increase in H/C ratios, with thermal cracking yielding more saturated liquid products than hydroconversion. In addition, both upgrading processes generate liquid products with reduced sulfur content, when

**Table 1. Elemental Composition<sup>a</sup> of Raw Asphaltenes and Their Hydroconversion and Thermal Cracking Products**

sample	raw asphaltenes	hydroconversion liquid products	thermal cracking liquid products
C (wt %)	82.96	82.50	82.42
H (wt %)	7.10	7.98	8.61
N (wt %)	1.03	0.93	0.83
S (wt %)	7.45	6.84	6.08
H/C	1.02	1.16	1.25

<sup>a</sup>The absolute errors of the elemental analysis measurements are between 0.02 and 0.04 wt %, and the standard errors of the mean are between 0.02 and 0.09.

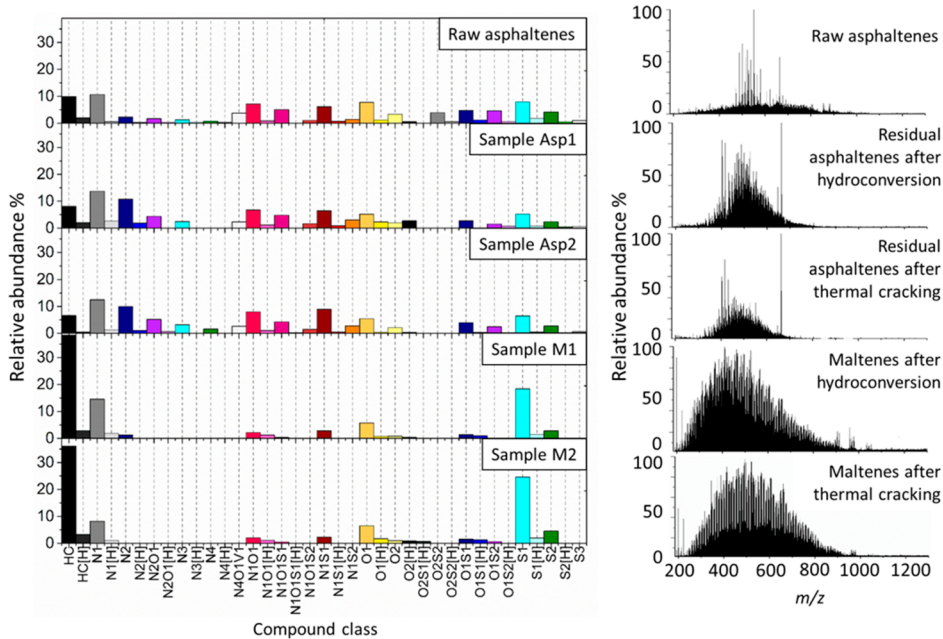


**Figure 2.** Compound class distributions and MWDs for raw asphaltenes and residual asphaltenes (Asp1, Asp2) and maltenes (M1, M2) after upgrading.

compared with the raw asphaltenes. Similarly, Purcell et al.<sup>11</sup> reported a decrease in sulfur content in the residual asphaltenes after hydroconversion and Liu et al.<sup>29</sup> observed an increase in H/C ratios, and a reduction in sulfur and nitrogen contents for hydrocracked Venezuelan asphaltenes. On the other hand, the elemental analysis of the unfractionated liquid products revealed nonsignificant changes in nitrogen content.

It is well-known that yields of coke, gases, residual asphaltenes, and maltenes in upgrading processes are a direct consequence of the feedstock composition and the reaction environment.<sup>35</sup> Although many analytical approaches have been used to trace feedstock fate and upgrading products composition, the complexity of these samples prevents in-depth compositional analysis by traditional spectroscopic methods.

Raw and residual asphaltenes (Asp1 and Asp2) and the new malene fractions (M1 and M2), from hydroconversion and thermal cracking processes, were analyzed by APPI (+) FT-ICR mass spectrometry under optimized conditions (see section S-I for ionization source conditions). Ion signals in the mass spectra were analyzed with the software Composer, using the Kendrick mass defect criteria for elemental composition assignment. Section S-III of the Supporting Information contains the number of elemental assignments for each sample, and the root-mean-square deviation (RMS) of the assignation error in parts per billion (ppb). Assignment errors fluctuate between 277 and 642 ppb; a RMS value of <700 ppb provides unequivocal elemental composition assignment for practically all compound classes.<sup>37,38</sup> However, special attention should be paid to elemental composition assignments of compound classes with high heteroatom content. For example, if there is more than one elemental composition for a signal, with a mass tolerance below 1 ppm, the assignment can be confirmed by looking at the isotopic fine structure.<sup>38</sup> On this subject, section S-II contains the quality control analysis of the FT-ICR MS data such as recalibration status of the mass spectra, assignment performance and isotopic patterns for heteroatom-containing

compound classes. Regarding the number of molecular assignments, one can conclude that sample polydispersity was reduced after upgrading, because of the low number of elemental compositions found in the malene fraction, when compared with the starting material. Similarly, Purcell et al.<sup>11</sup> reported a decreased number of elemental assignments in Iraqi asphaltenes after hydroconversion.

Figure 2 shows the compound class distribution and the mass spectra for the raw asphaltenes and the samples Asp1, Asp2, M1 and M2. The molecular weight distributions (MWDs) of maltenes suggest profound transformations of the asphaltene feedstock through hydroconversion and thermal cracking processes. While the feedstock exhibits a MWD of  $220 < m/z < 980$ , centered around  $m/z$  600, compounds on M1 and M2 samples are shifted to lower masses with MWDs of  $200 < m/z < 920$ , centered around  $m/z$  420 and  $m/z$  490 for maltenes after hydroconversion and thermal cracking, respectively. Residual asphaltenes have also different mass spectral profiles than the original asphaltenes. Asp1 and Asp2 MWDs are  $300 < m/z < 800$ , and both are centered on  $m/z$  500.

Sorting molecular assignments in compound classes provides a different vantage point to observe the effect of the upgrading processes on the asphaltene feedstock. Figure 2 displays the compound class distribution of the samples, presented as the relative abundance of each class, detected as either, or both, radical cations and protonated molecules. The raw asphaltenes exhibit 21 compound classes: HC, N<sub>1</sub>, N<sub>2</sub>, N<sub>2</sub>O<sub>1</sub>, N<sub>3</sub>, N<sub>4</sub>, N<sub>4</sub>O<sub>1</sub>V, N<sub>1</sub>O<sub>1</sub>, N<sub>1</sub>O<sub>1</sub>S<sub>1</sub>, N<sub>1</sub>O<sub>1</sub>S<sub>2</sub>, N<sub>1</sub>S<sub>1</sub>, N<sub>1</sub>S<sub>2</sub>, O<sub>1</sub>, O<sub>2</sub>, O<sub>2</sub>S<sub>1</sub>, O<sub>2</sub>S<sub>2</sub>, O<sub>1</sub>S<sub>1</sub>, O<sub>1</sub>S<sub>2</sub>, S<sub>1</sub>, S<sub>2</sub>, and S<sub>3</sub>. The same trend in compound class distribution and relative abundances is observed for the residual asphaltenes (Asp1 and Asp2), except for the classes O<sub>2</sub>S<sub>1</sub> and O<sub>2</sub>S<sub>2</sub>, which are only detected in the raw sample. In contrast, maltenes' composition is very different to that of the raw asphaltenes. After hydroconversion, only 9 compound classes are detected in maltenes (HC, N<sub>1</sub>, N<sub>2</sub>, N<sub>1</sub>O<sub>1</sub>, N<sub>1</sub>S<sub>1</sub>, O<sub>1</sub>, O<sub>1</sub>S<sub>1</sub>, S<sub>1</sub>, and S<sub>2</sub>), while maltenes from thermal cracking exhibit the following compound classes: HC, N<sub>1</sub>, N<sub>1</sub>O<sub>1</sub>, N<sub>1</sub>S<sub>1</sub>, O<sub>1</sub>, O<sub>2</sub>,

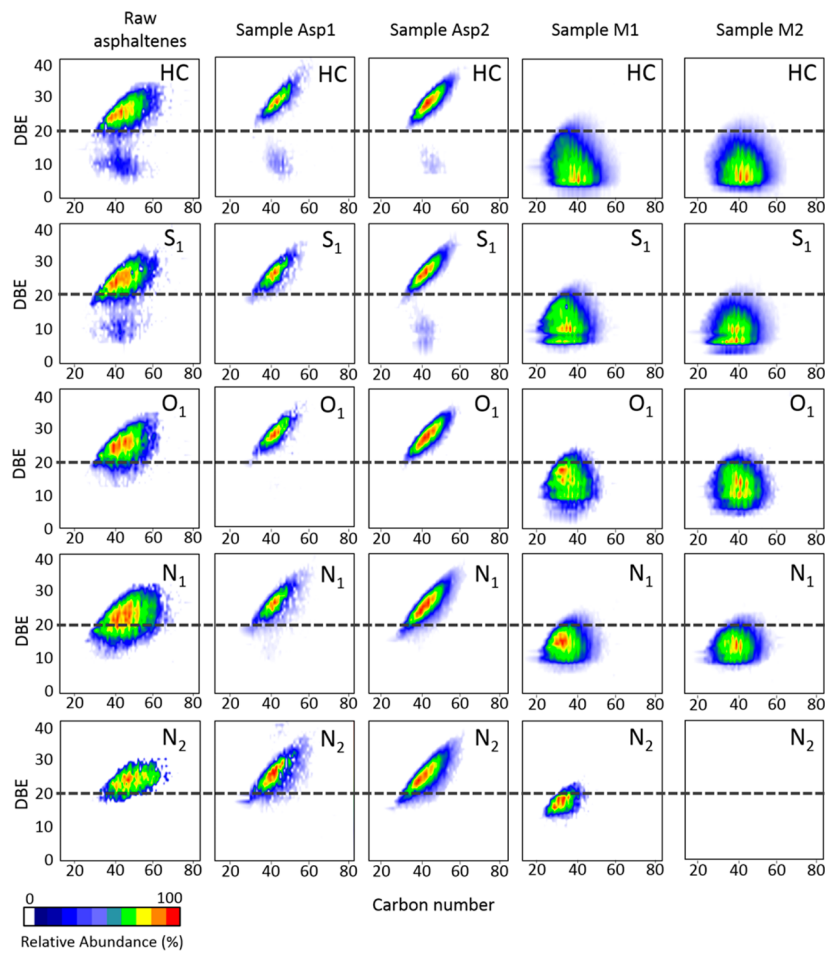


**Figure 3.** DBE versus carbon number plots for HC, S<sub>1</sub>, O<sub>1</sub>, N<sub>1</sub>, and N<sub>2</sub> compound classes in raw asphaltenes and residual asphaltenes (Asp1 and Asp2) and maltenes (M1 and M2) after upgrading.

O<sub>1</sub>S<sub>1</sub>, S<sub>1</sub>, and S<sub>2</sub>. Interestingly, the class HC, or hydrocarbons with no heteroatoms, is the most abundant (~35%–40%) in maltenic fractions M1 and M2, although this compound class has very low abundance in the starting asphaltenic material (~10%). These results indicate the suitability of hydroconversion and thermal-cracking processes to yield products enriched with useful hydrocarbons (of the HC kind), from Colombian asphaltenes.

Regarding the molecular composition of produced maltenes after upgrading, the absence of compound classes with high heteroatom content, such as N<sub>2</sub>O<sub>1</sub>, N<sub>3</sub>, N<sub>4</sub>, N<sub>1</sub>O<sub>1</sub>S<sub>2</sub>, N<sub>1</sub>S<sub>2</sub>, O<sub>2</sub>S<sub>2</sub>, O<sub>1</sub>S<sub>2</sub>, and S<sub>3</sub>, and the prevalence of the classes HC, N<sub>1</sub>, N<sub>2</sub>, N<sub>1</sub>O<sub>1</sub>, N<sub>1</sub>O<sub>1</sub>S<sub>1</sub>, N<sub>1</sub>S<sub>1</sub>, O<sub>1</sub>, O<sub>2</sub>, O<sub>1</sub>S<sub>1</sub>, S<sub>1</sub>, and S<sub>2</sub> with less heteroatoms could be indicative of nitrogen and sulfur loss from the raw asphaltenes. Similarly, an increase in the relative abundance of the classes HC and S in the maltenic products suggests that heteroatomic classes undergo breakup reactions where some N moieties and S moieties are lost, giving rise to simpler hydrocarbons.<sup>39</sup> Supporting these observations, Purcell et al.<sup>11</sup> used FT-ICR MS to follow the compositional changes in Iraqi asphaltenes during deep hydroconversion and reported a sequential loss of S atoms from classes such as S<sub>3</sub> and N<sub>1</sub>S<sub>3</sub> to produce S<sub>2</sub> and N<sub>1</sub>S<sub>2</sub> classes, respectively. In another work, Gray et al.,<sup>40</sup> who performed hydrocracking of heavy residues from Alberta bitumen, concluded that the conversion of asphaltenes occurs mostly through cracking of long aliphatic

chains from the aromatic cores, with loss of heteroatoms such as sulfur (in sulfide-like functionalities).

Regarding sulfur-containing compounds, it is also important to consider that, under thermal cracking and hydroconversion conditions, alkyl sulfides would more likely turn into H<sub>2</sub>S and paraffins than thiophenic moieties.<sup>41</sup> Consequently, it could be feasible to assume that sulfur-containing families in produced maltenes or in residual asphaltenes are most likely present in the form of thiophenic functionalities. In this regard, Hauser et al.<sup>9</sup> reported that sulfides in saturates or as side chains in aromatics, resins, and asphaltenes, are more likely to undergo thermal cracking reactions than thiophene moieties. The authors studied vacuum residues reactivity under thermal cracking conditions and suggested that nonthiophenic sulfur is removed from the feedstock and transformed to H<sub>2</sub>S, which is detected in the produced gases in high concentrations (14 wt %). On the other hand, we found that refractory sulfur present in thiophenic functionalities is resistant to conversion, and remains concentrated in the residual pitch. Supporting these observations, Jimenez et al.,<sup>42</sup> using X-ray photoelectron spectroscopy, studied coke samples from the carbonization reaction of a Maya vacuum residue and found thiophenic sulfur to be the most abundant functionality.

Histograms of compound class distribution in Figure 2, although useful as a general way to compare sample composition, do not contain detailed molecular information. Thus, data analysis by graphic methods such as isoabundance-

contoured plots of double bond equivalents (DBEs) versus carbon number, are useful to follow asphaltenes molecular changes after upgrading.<sup>11,43</sup> Figure 3 shows the isoabundance-contoured plots of DBE versus carbon number for the compound classes HC, S<sub>1</sub>, O<sub>1</sub>, N<sub>1</sub>, and N<sub>2</sub> for the raw asphaltenes and for the residual asphaltenes (Asp1 and Asp2) and maltenes (M1 and M2) obtained after hydroconversion and thermal cracking. The plots are normalized to the highest signal abundance for each class. Raw asphaltenes are highly aromatic compounds with DBE values ranging from 18 to 33, and carbon numbers between 30 and 65. On the other hand, contoured plots of DBE versus carbon number for samples M1 and M2, the maltenes product of hydroconversion and thermal cracking processes, exhibit significant differences when compared to the original and residual asphaltenes. Maltenes in Figure 3 have low DBE values (<22) and carbon numbers between 20 and 60. This distribution is quite similar to that reported by McKenna and co-workers for vacuum distillation cuts (371–510 °C and 510–538 °C) of a Middle Eastern heavy crude oil.<sup>44</sup>

Generally speaking, the composition of the residual asphaltenic and maltenic fractions after upgrading reflects the chemical complexity of the starting material. After upgrading, DBE values for residual asphaltenes range from 22 to 37, with carbon numbers from 32 to 56, in contrast with the values for the original sample (DBE from 18 to 33 and carbon numbers from 30 to 65). We observe no significant differences between the contoured plots for residual asphaltenes from hydroconversion and thermal cracking processes. The slight increase in DBE in residual asphaltenes after upgrading, with little reduction in carbon number, can be associated with dehydrogenation of peripheral naphthenic rings in the asphaltene core structure, as has been previously reported. For example, Ancheyta et al.<sup>27</sup> reported that hydrotreated asphaltenes increase their aromaticity factors, in comparison with the feedstock; and similar trends have also been observed by Rodgers et al.<sup>11</sup> On the other hand, regarding changes in molecular structure during upgrading, Koinuma et al.<sup>45</sup> reported that, below 400 °C, in thermal cracking processes, cleavage of alkyl side chains occurs mainly without altering the asphaltene's core. Hence, under thermal and hydroconversion conditions in our experiments (430 °C), we could hypothesize that conversion of asphaltene's structure begins with a loss of alkyl side chains with further modification of the aromatic core structure. According to Figure 3, the original asphaltene sample consist of molecules with aromatic cores containing up to 30 carbon atoms in their alkyl side chains, while residual asphaltenes are mostly condensed units with few alkyl groups, where the most abundant homologous series only have up to 18 methylene units in their structures. Plots of DBE versus carbon number provide a way to calculate an approximate number of carbon atoms in the alkyl side chains of asphaltenes. For instance, let us consider the molecular species located at the planar limit in the DBE versus carbon number plots, which correspond to the beginning of each homologous series. Each point in these homologous series (moving horizontally from left to right) indicates the addition of one carbon atom to the alkyl side chains, attached to the core structure. In other words, raw asphaltenes consist of aromatic cores having at least 30 carbon atoms in the alkyl side chains.

The observation of narrow distributions along the homologous series in the residual asphaltenes in Figure 3 suggests a massive loss of alkyl chains from the original asphaltene sample.

Along the same lines, Chiaberge et al.,<sup>46</sup> using NMR and FT-IR, concluded that thermal cracking of asphaltenes proceeds through reactions based on radical fragmentation, producing dealkylation and peripheral naphthenic unit aromatization. In another report, Kawai et al.<sup>47</sup> presented a mechanism for thermal cracking of heavy oils where asphaltene dealkylation is a consequence of free radicals attacking the asphaltene structure; in this fashion, dealkylation reactions produce asphaltenes with smaller sizes. An alternative reaction pathway involves radical recombination to produce highly condensed asphaltenes, with few alkyl side chains, commonly associated with coke production.

Until this point, we could argue that residual asphaltenes must consist of highly condensed and very stable "cores", left after the cleavage of alkyl chains from the original asphaltenes, which are able to survive the upgrading process. This idea coincides with abundant reports in the literature depicting asphaltenes as thermally stable polycyclic aromatic molecules with alkyl side chains or peripheral naphthenes. Both alkyl and naphthenic groups in these structures are cracked in thermal or catalytic upgrading, while the remaining aromatic cores may undergo further reactions to produce coke.<sup>48</sup> Along these lines, the produced maltenes, essentially the *n*-C<sub>7</sub> soluble fraction of the cracked products, must also contain information about the structure of the raw asphaltenes. This train of thought was the basis for a report by Gray et al.,<sup>30</sup> where analysis by GC-FD-TOF of the distillable fraction from hydrocracked asphaltenes showed that basic units in asphaltenes could consist of 1-, 2-, 3-, 4-ring naphthenes, 1-, 2-, 3-ring aromatics with thiophene functionalities, and 4+-ring aromatic units. In our case, the DBE versus carbon number plots for maltenes in Figure 3 indicate a large diversity of building blocks in the starting material. For example, the HC class, which is the most abundant in maltenes, has compounds with DBE values between 4 and 12 that might be indicative of structures consisting of 1–4-ring aromatics with up to 20 carbon atoms in their alkyl side chains.<sup>49</sup>

Regarding class N<sub>1</sub> in samples M1 and M2, molecular species with DBE values of 14–15 and carbon number between 30 and 36 exhibit the highest abundances. According to Purcell et al.,<sup>50</sup> nitrogen-containing aromatics under APPI conditions can form radical cations (if the N is contained within a pyrrolic moiety), and protonated molecules (if the N is pyridinic). We observe a high abundance of radical cations in M1 and M2 samples, which indicate the presence of pyrrolic units. Supporting this assumption, Purcell et al.<sup>50</sup> reported high abundance of pyrrolic functionalities with DBE values of 14–15 in South American crude oils analyzed by APPI + FT-ICR and suggested the presence of dibenzocarbazoles in the samples. Along the same lines, the N<sub>1</sub> class in residual asphaltenes is detected as radical cations in high abundance. It is important to note that nitrogen moieties in the residual asphaltic material must be embedded in large and highly condensed aromatic cores with few alkyl side chains.

In the case of oxygen, the petroleome of class O<sub>1</sub> in raw asphaltenes spans from DBE = 18 to DBE = 33, increasing slightly in the residual asphaltenes (from DBE = 22 to DBE = 35); and carbon numbers in the raw asphaltenes go from 30 to 65, decreasing slightly in the residuals (carbon numbers go from 32 to 55). Mullins<sup>51</sup> has suggested that the oxygen content in asphaltenes is low, in comparison to sulfur, and that O<sub>1</sub> may be present in polar groups such as phenols and furans. In the residual asphaltenes from both upgrading processes, the O<sub>1</sub> class presents a molecular composition with DBE values

slightly increased and reduced number of methylene units, when compared with the starting material. On the other hand, the low aromaticity of the O<sub>1</sub> class in produced maltenes contrasts with the high aromaticity of the asphaltene feedstock. In maltenes, DBE values for the O<sub>1</sub> class range from 8 to 22 with alkylation up to 22 methylene units, suggesting a wide variety of elementary units in the starting material.

The N<sub>2</sub> class in residual asphaltenes, presents a slightly increase in DBE values and lower content of methylene units than the raw asphaltenes. Nitrogen in residual asphaltenes must be present as pyrrolic or pyridinic moieties within the aromatic core structure.<sup>52,53</sup> On the other hand, N<sub>2</sub> class in produced maltenes after hydroconversion, exhibits a narrow molecular distribution with DBE values between 12 and 22 and a methylene content of up to 18 units.

One of the main concerns in upgrading schemes is related to sulfur content in the products, which not only affects the fuel price but also has a negative impact in the atmosphere, where it is released as SO<sub>x</sub> after combustion.<sup>12</sup> The S<sub>1</sub> compound class in maltenes from hydroconversion and thermal cracking displays a bimodal distribution, as seen in Figure 3. The plot of the DBE distribution for this compound class in Figure 4

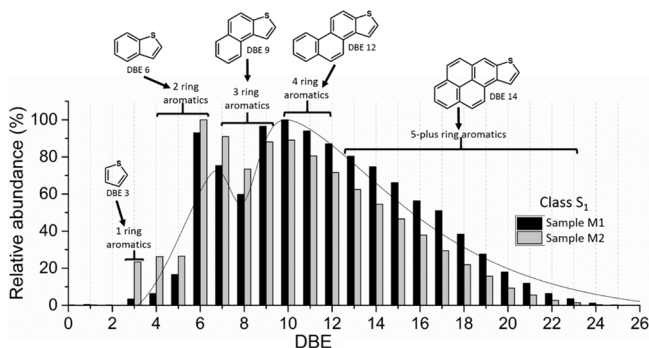


Figure 4. DBE distribution for the S<sub>1</sub> class in maltenes (M1 and M2) after hydroconversion and thermal cracking processes.

clearly shows two series. The first homologous series has a maximum at DBE = 6, which extends along carbon numbers 20 to 54, while the second series presents a maximum at DBE = 10 and spans from carbon numbers 18 to 56. Regarding sulfur molecules in products from hydrocracked asphaltenes, Gray et al.,<sup>30</sup> using gas chromatography coupled to FI-TOF-MS, found that cracked sulfur-containing products consist mostly of 2-ring (benzothiophenes) and 3-ring aromatics (naphthenobenzothiophenes and dibenzothiophenes), among other products such as sulfides. Using data from the literature, in Figure 4, we include a set of S<sub>1</sub> aromatic model molecules as illustration. While studying the molecular composition of a Venezuelan vacuum residue by theoretical calculations and FT-ICR MS, Zhang et al.<sup>54</sup> reported that S<sub>1</sub> species with DBE distribution between 3 and 25 are probably thiophenic, while sulfides must have DBE values below 5. In another report, Liu et al.<sup>55</sup> using FT-ICR MS observed that sulfide compounds in petroleomes are usually located in the low DBE region (DBE < 4) while sulfur in thiophenic functionalities is part of the molecules with DBE values of >4. In addition, Hauser et al.<sup>9</sup> indicated that a thermal cracking of sulfides is more probable than conversion of thiophenic functionalities. Along these lines, sulfur species in produced maltenes, of the S<sub>1</sub> type, may consist mostly of thiophenic structures. Figure 4 suggest abundant building

blocks based on mono-, di-, and tri (and plus)-benzothiophenic structures, with alkylation up to 30 methylene units in accordance with Figure 3. A possible sulfur-containing building block could be benzothiophene (DBE = 6). The addition of one and two fused aromatic rings to benzothiophene produces dibenzothiophene (DBE = 9) and benzonaphthothiophene (DBE = 12), respectively. S<sub>1</sub> compounds with DBE = 7 are likely benzothiophenes with one fused cycloalkane ring. Along these lines, the S<sub>1</sub> class species with DBE = 10 correspond to dibenzothiophenes with one fused cycloalkane ring.

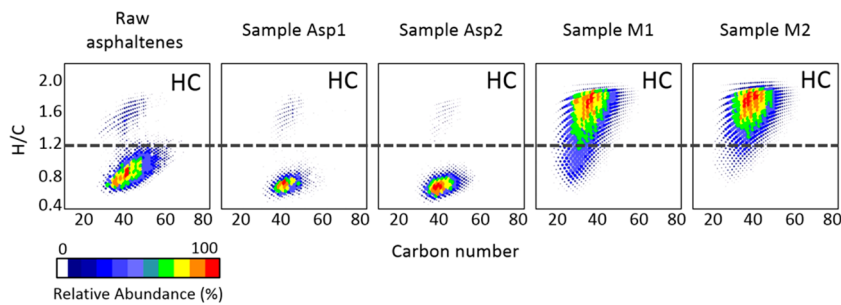
Additional structural information, in the form of the planar aromatic limits, can be derived from the DBE versus carbon number plots. Defined as the lines resulting from connecting maximum DBE values at a given carbon number,<sup>56,57</sup> the planar limit (particularly the slope of the lines) has been used for structural elucidation of fossil hydrocarbons.<sup>57,58</sup> Generally speaking, the planar limit slope corresponds to ~0.25 for saturated cyclic compounds, ~0.75 for catacondensed aromatic structures and ~0.90 for pericondensed aromatic structures.<sup>57</sup> The maximum value for the slope, according to the “90% rule”, is 0.90; this means that the maximum DBE value for a fossil hydrocarbon cannot exceed the 90% of its carbon content.<sup>58</sup> Section SIV in the Supporting Information contains several examples of planar limit calculations. Table 2 includes the slope

Table 2. Planar Aromatic Limit Slopes for Raw Asphaltenes, Residual Asphaltenes, and Produced Maltenes

class	Planar Aromatic Limit Slope				
	raw asphaltenes	Asp1	Asp2	M1	M2
HC	0.671	0.675	0.696	0.575	0.595
S <sub>1</sub>	0.614	0.635	0.684	0.694	0.560
O <sub>1</sub>	0.645	0.767	0.749	0.709	0.610
N <sub>1</sub>	0.595	0.711	0.646	0.658	0.645
N <sub>2</sub>	0.578	0.764	0.667	0.444	---

of the planar limits for the HC, S<sub>1</sub>, O<sub>1</sub>, N<sub>1</sub>, and N<sub>2</sub> compound classes in raw, residual asphaltenes (Asp1 and Asp2) and produced maltenes (M1 and M2). For classes S<sub>1</sub>, O<sub>1</sub>, N<sub>1</sub>, and N<sub>2</sub>, the planar limit slopes are significantly higher for the residual asphaltenes than for the raw material, indicating a general structural change toward more condensed aromatic architectures in the residual asphaltic material for these families. Importantly, compounds with the highest relative abundance in residual asphaltenes (in Figure 3) are clustered toward the planar aromatic limit, suggesting the prevalence of highly condensed aromatic species with little alkyl substitution after upgrading. In addition, O<sub>1</sub> compounds in Asp1 and Asp2 samples are the most condensed structures with the highest planar limit slopes. This fact suggests that hydroconversion produces O-containing residual asphaltenes that are more structurally condensed, when compared with the thermal cracking products.

On the other hand, class HC in maltenes, besides being the most abundant compound class in samples M1 and M2, presents planar limit slopes that are drastically reduced in comparison with the original asphaltenes. As discussed above, produced maltenes are enriched with hydrocarbons having low DBE values and high content of -CH<sub>2</sub> units (Figure 3). Considering planar limit slopes of 0.575 and 0.595 for M1 and M2, lower than the slope for original asphaltenes of 0.685, compounds in the maltene fraction may have molecular architectures consisting of a combination of alkyl chains with



**Figure 5.** H/C versus carbon number plots for the HC class in raw asphaltenes, and residual asphaltenes (Asp1 and Asp2) and maltenes (M1 and M2) after upgrading.

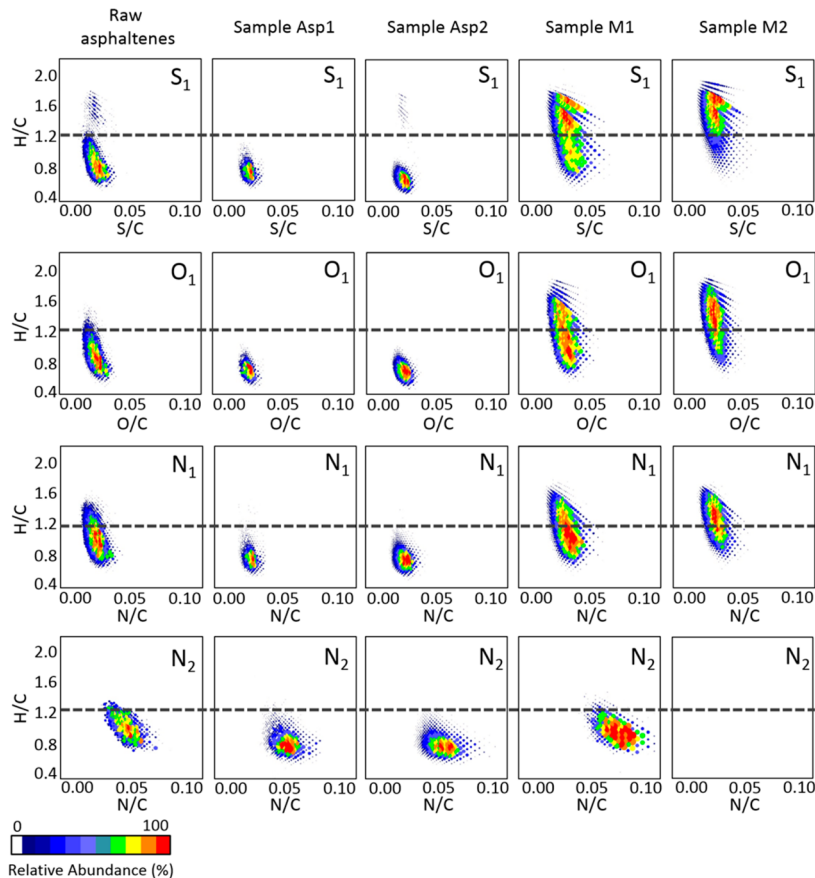


**Figure 6.** van Krevelen diagrams for classes HC, S<sub>1</sub>, O<sub>1</sub>, N<sub>1</sub>, N<sub>2</sub> in raw asphaltenes, and residual asphaltenes (Asp1 and Asp2) and maltenes (M1 and M2) after upgrading.

aromatic or naphthenic units linearly added, as previously indicated by Cho et al.<sup>57</sup> We believe that the analysis of planar limit slopes could give us a hint as to the structure of the original asphaltenes. For example, the observed decline in planar limit slopes for the HC family, in contrast with the original asphaltenes, indicates that, after upgrading, the HC family has a more linear architecture than the starting material. Structurally speaking, this observation hints the existence of island-type structures from which linear structures (maltenes) and condensed aromatic cores (residual asphaltenes) arise after upgrading. Interestingly, the behavior of the N<sub>1</sub> class in maltenes is contrary to that of the HC class. For the N<sub>1</sub> class, we observe increased planar limit slopes of 0.658 and 0.645 for samples M1 and M2, respectively, in contrast with the original asphaltene planar limit slope of 0.595. The behavior is similar

for residual asphaltenes with slopes of 0.711 and 0.646 for Asp1 and Asp2, respectively. The increment in planar limit slope indicates that, after upgrading, the N<sub>1</sub> compound family in maltenes has a higher condensed architecture than the starting material; structurally speaking, this observation only agrees with an original structure (from which the N<sub>1</sub> family in maltenes arises) having archipelago architecture. However, these conclusions are not as straightforward for compound classes S<sub>1</sub> and O<sub>1</sub>. Although, for S<sub>1</sub> and O<sub>1</sub> classes in residual asphaltenes, planar limit slopes always increase, in comparison with the original asphaltene sample, which suggests a shift toward pericondensed aromatic architectures, no definite conclusion can be drawn about the architecture of these families in maltenes.

An alternative method to display compositional information for complex mixtures is provided by the van Krevelen diagrams. In this regard, several groups of researchers<sup>33,59–61</sup> have analyzed supercomplex hydrocarbons mixtures using two- and three-dimensional van Krevelen plots. These molecular representations, which are constructed by plotting H/C versus O/C (or N/C or S/C) atomic ratios, are extremely useful in interpreting FT-IRC MS data. They have also been used for visual analysis of petrochemical samples from diverse origin, maturity, and processing, and for other complex mixtures, such as natural organic matter, lignin, and humic acids.<sup>59,60</sup> Strictly speaking, the HC class cannot be displayed in a van Krevelen diagram; however, a modified version of the diagram can be built in terms of H/C ratios versus carbon number. Figure 5 shows the H/C versus carbon number plots for the HC class present in the raw asphaltenes, and in the residual asphaltenes (Asp1, Asp2) and the produced maltenes (M1, M2) after upgrading. In contrast with raw asphaltenes showing H/C ratios between 0.60 and 1.20, residual asphaltenes exhibit the lowest H/C ratios in all samples, with values ranging from 0.50 to 0.85 for the hydrotreated samples and from 0.46 to 0.85 for the thermal cracked samples. Also, it is possible to visualize that the carbon number is reduced, from 30–65 in the raw asphaltenes, to 33–55 for the hydrotreated and 32–58 for the thermal cracked residual asphaltenes. In this sense, raw asphaltenes consist of more alkylated molecules (~35 methylene units), when compared with the residual asphaltic compounds (with ~18 methylene units). This means the upgrading procedures dramatically transform the feedstock, leaving behind highly aromatic and relatively small molecules with fewer alkyl units in their structures as residues. Merdrignac et al.<sup>28</sup> used NMR to study molecular changes in asphaltenes upon hydroconversion processes. Lower CH<sub>2</sub>/CH<sub>3</sub> ratios were found in residual asphaltenes, compared with the feedstock, suggesting that remaining asphaltenes consist of aromatic cores with fewer CH<sub>2</sub> units, which indicates alkyl chain length reduction.

The maltenes fraction, produced after upgrading, exhibits the highest H/C ratios in all samples, with values ranging from 0.80 to 1.82 for the hydrotreated and from 0.95 to 2.00 for the thermal cracked. Also, the carbon number is reduced from 30–65 in the raw asphaltenes, to 20–50 in the hydrotreated and 20–55 in the thermal cracked maltenes, which suggests that maltenic products are smaller and more saturated than the asphaltene feedstock. Interestingly, by combining information on planar limit slopes and van Krevelen diagrams, we could strengthen some previous conclusions regarding structural information for the HC class. For example, let us consider the original asphaltene sample with a high abundance of molecular species around a H/C ratio of 0.8, the residual asphaltenes with abundant species with H/C ratio of 0.6 and the maltenes with high abundance of species with H/C 1.8. The HC family in maltenes from the upgrading process exhibits H/C ratios much higher than the original or residual asphaltenes, indicating highly saturated, and probably linear, structures composed of naphthenic units with high alkyl content, in agreement with our previous observation of low planar limits for this compound class. The high linearity and saturation of this fraction could imply its provenance mostly from island-type structures in the original feedstock.

Concerning compound classes containing heteroatoms, Figure 6 shows the van Krevelen diagrams for classes S<sub>1</sub>, O<sub>1</sub>, N<sub>1</sub>, and N<sub>2</sub> in the raw feedstock, and in the residual asphaltenes

(Asp1, Asp2) and maltenes (M1, M2) after upgrading. In these diagrams, homologous series of compounds correspond to diagonals intersecting in H/C = 2 with alkylation increasing from right to left along the line. Clearly the heteroatom-containing families in maltenes share some of the compositional space of the original asphaltenes. However, in samples M1 and M2, we observe an increase in signal abundance for species with high H/C ratios, in contrast with the original asphaltene sample. This effect is more pronounced in S<sub>1</sub>, N<sub>1</sub>, and O<sub>1</sub>-containing maltenes from thermal cracking, and particularly for the S<sub>1</sub> class. Interestingly, heteroatom-containing maltenes that have high H/C content or are more saturated (upper left corner of the van Krevelen diagrams for samples M1 and M2) are “bigger”, in terms of number of carbon atoms, than the same species that have a low H/C content (lower right corner of the diagrams for M1 and M2), and are less saturated and “smaller”. On the other hand, when compared with the HC class compositional space (Figure 5), the S<sub>1</sub>, N<sub>1</sub>, and O<sub>1</sub>-containing maltenes are shifted to lower H/C ratios, meaning that heteroatom-containing species have a more aromatic nature than the HC class in maltenes. This behavior also supports the conclusions derived from the analysis of the DBE vs carbon number plots (see Figures 3 and 4), where we pointed out that S-containing species could be homologous series of mono-, di-, tri-, and tetra-benzothiophenes. However, it is important to point out that S<sub>1</sub>, O<sub>1</sub>, and N<sub>1</sub> molecules in maltenes exhibit higher H/C ratios than the raw asphaltenes, also with a dramatic decrease in carbon number. For example, the average carbon number in the starting material is ~50 (N/C or O/C = 0.020), whereas for maltenes after hydroconversion, the carbon number is ~30 (N/C or O/C = 0.033) and for maltenes after thermal cracking, the carbon number is ~38 (N/C or O/C = 0.026). Along the same lines, the N<sub>2</sub> family, which is detected in maltenes after hydroconversion but not in maltenes after thermal cracking, has H/C ratios quite similar to the asphaltene feedstock. However, in this family, the carbon number is dramatically reduced from an average of ~40 (N/C = 0.050), in the starting material, to an average of ~25 (N/C = 0.080) in hydroconversion maltenes. Regarding the molecular composition of the residual asphaltenes, van Krevelen diagrams confirm that hydroconversion and thermal cracking yield asphaltic material with higher hydrogen deficiency than the feedstock, which could be originated from dealkylation and dehydrogenation reactions on peripheral naphthenic rings in the asphaltene core structure, as discussed previously.<sup>62</sup> As with the previous HC class, van Krevelen diagrams also support the conclusions reached when analyzing planar limit slopes for heteroatomic classes. For example, for the N<sub>1</sub> family, we observe a great abundance of molecular species at a H/C ratio of ~1.1 for raw asphaltenes, abundant species with a H/C ratio of 0.6 for residual asphaltenes, and maltenes with high abundance of species have a H/C ratio of 1.2. The N<sub>1</sub> family in maltenes from the upgrading process exhibits H/C ratios that are quite similar to those of the original asphaltenes. The only explanation for this observation is the existence of archipelago structures that upon cracking would produce fragments with the same H/C ratios as the original structure. These resulting structures are more “condensed” than the original molecule and, hence, would exhibit higher planar limits than the parent structure, just as we reported in Table 2.

Although the effect of hydroconversion and thermal cracking on the asphaltene feedstock generally is similar for most

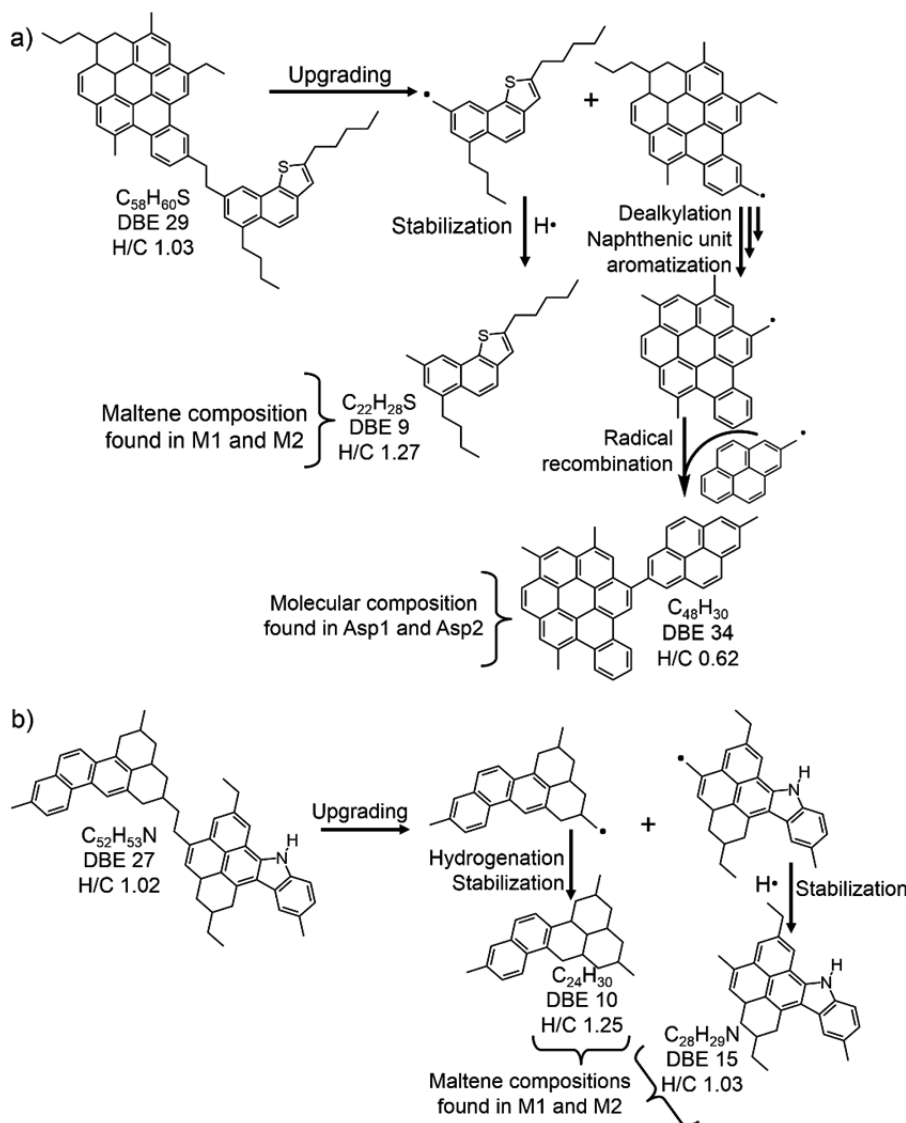


**Figure 7.** Hypothetical reaction pathways of model raw asphaltenes under hydroconversion or thermal cracking conditions: (a) island-type structure with dibenzothiophene substituent producing molecular compositions present in residual asphaltenes and produced maltenes; (b) archipelago-type structure producing maltenic products.

compound classes, O<sub>1</sub> and S<sub>1</sub> families do not exhibit the same behavior, and we believe they undergo different reaction pathways in both processes. In the case of thermal cracking, after the process, the planar limit slope decreases from 0.614 to 0.560 and from 0.645 to 0.610 for S<sub>1</sub> and O<sub>1</sub> families, respectively, while H/C ratios increase notably, in comparison with the hydroconversion process. These results suggest that thermal cracking produces highly saturated S<sub>1</sub>- and O<sub>1</sub>-containing compounds with structures probably consisting of fused linear naphthenic units primarily. On the other hand, hydroconversion yields S<sub>1</sub> and O<sub>1</sub> classes with higher planar limit slopes than the starting material—from 0.614 to 0.694 for S<sub>1</sub> class and from 0.645 to 0.709 for O<sub>1</sub> class, and lower H/C ratios than the thermal cracking products. This observation means that hydroconversion induces the production of less-saturated maltenic compounds (for the S<sub>1</sub> and O<sub>1</sub> families) with a more-condensed molecular architecture, when compared with the thermal cracking products.

At this point, it is important to highlight the usefulness of combining information derived from DBE versus carbon

number plots and van Krevelen diagrams. Separately, these graphs illustrate molecular features such as DBEs, the number of methylene units in the structure, H/C ratios, and carbon numbers; however, together, they are extremely useful to establish reactivity trends of compound families under hydroconversion and thermal cracking processes, as well as structural features of the asphaltene feedstock. As stated above, after upgrading, highly saturated HC with a slightly condensed architecture are produced. On the other hand, upgrading yields N<sub>1</sub> maltenic compounds with a higher degree of molecular condensation and H/C ratios that are similar to those of the starting material; however, S<sub>1</sub> and O<sub>1</sub> classes seem to undergo different reaction pathways. These results indicate the existence of diverse architectures whose transformation, by several routes, results in the products that we observe.<sup>63</sup> Several reports indicate that the transformation of asphaltenes under hydroconversion or thermal cracking conditions begins with the loss of alkyl side chains from the island-type aromatic structures, followed by modification of peripheral naphthenic rings in the aromatic core.<sup>46,62,64</sup> On the other hand, some groups report

archipelago-type structures undergoing breakage of the aliphatic linkages between the aromatic moieties to give lighter products than the starting asphaltic compounds.<sup>36,65,66</sup> In this sense, the molecular composition of the residual asphaltenes and the produced maltenes in our experiments suggest the coexistence of island-type and archipelago-type structures in the raw asphaltene sample. This observation is not new and has been previously reported by Rodgers et al.,<sup>61</sup> who performed FT-ICR MS/MS analysis of asphaltenes and found that their molecular structures display island-type and archipelago-type structural motifs.

We hypothesize that, under hydroconversion and thermal cracking conditions, highly stable heteroatomic island-type structures undergo a loss of alkyl side chains and aromatization of peripheral naphthenic rings. As a result, residual asphaltenes show increased DBE values and a dramatic decrease in alkylation, while the produced maltenes have low DBE values, abundant methylene units, and high H/C ratios, when compared to the original asphaltenes. According to our observations, compound classes HC and S<sub>1</sub> in produced maltenes (see Figures 3, 5, and 6) could originate through this process. On the other hand, heteroatomic archipelago-type structures undergo excision of linkages between aromatic moieties, producing mostly lighter heteroatom-containing maltenic compounds with a slight increase in H/C ratios, and structures with a relative high number of methylene units and reduced DBE and carbon numbers, when compared with the raw asphaltenes. Compound classes N<sub>1</sub> and N<sub>2</sub> in produced maltenes (Figures 3, 5, and 6) could arise from this process, while compound class O<sub>1</sub> exhibits an intermediate behavior.

Figure 7 depicts, solely with an illustrative purpose, the possible reaction routes of the raw asphaltenes transformation to produce maltenic compounds and residual asphaltenes, under the assumptions exposed above. All structures in Figure 7 have a molecular composition that is contained within the petroleomes of Figures 3, 5, and 6.

## CONCLUSIONS

Sorting high-resolution mass spectrometry data in compound class distributions is useful to observe general trends in compositional changes when asphaltenes undergo upgrading processes. More specific information is derived from plots of DBE versus carbon number, which suggest that, under thermal cracking and hydroconversion conditions, asphaltenes produce two types of compounds: one consisting of highly condensed and very stable aromatic cores with little alkyl substitution, classified as residual asphaltenes (insoluble in *n*-heptane); and another composed by molecules with lower DBE values and lower carbon numbers than the feedstock, classified as maltenes (soluble in *n*-heptane). In addition, from these plots, structural information is also derived in the form of planar limit slopes, which are related to the degree of condensation of the molecular structure. In this sense, the maltenic fractions after upgrading have hydrocarbons (HC class) with low aromatic condensation. In contrast, N<sub>1</sub>-containing structures seem to be more condensed. On the other hand, residual asphaltenes invariably exhibit a shift toward more-condensed architectures.

In addition, we can also have some insight into the original asphaltene structure as the petroleomes of the residual asphaltenic and maltenic fractions after upgrading reflect the starting material composition. For instance, we hypothesize that some raw asphaltenes with island-type structures, having “arms” or side chains made of alkyl units or mono-, di-, or tri-

benzothiophene units, undergo upgrading to form the HC and S<sub>1</sub> compounds that are present in maltenes. These two classes exhibit high saturation, decreased structural condensation, lower carbon numbers, and dramatic decrease in aromaticity than both the original and the residual asphaltenes. Similarly, one can conclude that N<sub>1</sub>-containing compounds in produced maltenes are exclusively derived from archipelago-type structures. All of our observations suggest a parent asphaltene composed of a mixture of island-type and archipelago-type motifs.

## ASSOCIATED CONTENT

### Supporting Information

The Supporting Information is available free of charge on the ACS Publications website at DOI: [10.1021/acs.energyfuels.5b01510](https://doi.org/10.1021/acs.energyfuels.5b01510).

Atmospheric pressure photoionization source conditions for each sample; recalibration status, assignment performance, and isotopic pattern check for mass spectra of original asphaltenes, residual asphaltenes, and produced maltenes; number of elemental assignments and RMS of error (in ppb); and examples of planar limit slope calculation (PDF)

## AUTHOR INFORMATION

### Corresponding Author

\*Tel.: 57-76344000, ext 2215. Fax: 57-76459919. E-mail: [marianny@uis.edu.co](mailto:marianny@uis.edu.co).

### Notes

The authors declare no competing financial interest.

## ACKNOWLEDGMENTS

We acknowledge COLCIENCIAS and the Central Research Laboratory Facility at Guatiguará's Tech Park, Universidad Industrial de Santander, Piedecuesta-Santander, for a Graduate Fellowship and technical support, respectively. This work was also supported by the Research Agreement No. 5211770 between ECOPETROL S.A. and Universidad Industrial de Santander.

## REFERENCES

- (1) Aleklett, K.; Höök, M.; Jakobsson, K.; Lardelli, M.; Snowden, S.; Söderbergh, B. *Energy Policy* **2010**, *38*, 1398–1414.
- (2) Dorian, J. P.; Franssen, H. T.; Simbeck, D. R. *Energy Policy* **2006**, *34*, 1984–1991.
- (3) Bentley, R. W. *Energy Policy* **2002**, *30*, 189–205.
- (4) Shah, A.; Fishwick, R.; Wood, J.; Leeke, G.; Rigby, S.; Greaves, M. *Energy Environ. Sci.* **2010**, *3*, 700–714.
- (5) Dunn, J. a.; MacLeod, J. B.; Myers, R. D.; Bearden, R. *Energy Fuels* **2003**, *17*, 38–45.
- (6) Morimoto, M.; Sugimoto, Y.; Sato, S.; Takanohashi, T. *Energy Fuels* **2014**, *28*, 6322–6325.
- (7) Fahim, M.; Al-Sahhaf, T.; Elkilani, A. *Fundamentals of Petroleum Refining*; Elsevier: Amsterdam, 2009.
- (8) Jansen, T.; Guerry, D.; Leclerc, E.; Ropars, M.; Lacroix, M.; Geantet, C.; Tayakout-Fayolle, M. *Ind. Eng. Chem. Res.* **2014**, *53*, 15852–15861.
- (9) Hauser, A.; AlHumaidan, F.; Al-Rabiah, H.; Halabi, M. A. *Energy Fuels* **2014**, *28*, 4321–4332.
- (10) Rana, M. S.; Sámano, V.; Ancheyta, J.; Diaz, J. A. I. *Fuel* **2007**, *86*, 1216–1231.
- (11) Purcell, J. M.; Merdignac, I.; Rodgers, R. P.; Marshall, A. G.; Gauthier, T.; Guibard, I. *Energy Fuels* **2010**, *24*, 2257–2265.
- (12) Babich, I. V.; Moulijn, J. A. *Fuel* **2003**, *82*, 607–631.

- (13) Akbarzadeh, K.; Hammami, A.; Kharrat, A.; Zhang, D.; Allenson, S.; Creek, J.; Kabir, S.; Jamaluddin, A. J.; Marshall, A. G.; Rodgers, R. P.; Mullins, O. C.; Solbakken, T. Asphaltenes—Problematic but Rich Potential. *Oilfield Rev.* **2007**, *19* (2), 22–43.
- (14) Buenrostro-Gonzalez, E.; Groenzi, H.; Lira-Galeana, C.; Mullins, O. C. *Energy Fuels* **2001**, *15*, 972–978.
- (15) Liu, P.; Shi, Q.; Chung, K. H.; Zhang, Y.; Pan, N.; Zhao, S.; Xu, C. *Energy Fuels* **2010**, *24*, 5089–5096.
- (16) Acevedo, S.; Guzmán, K.; Labrador, H.; Carrier, H.; Bouyssiere, B.; Lobinski, R. *Energy Fuels* **2012**, *26*, 4968–4977.
- (17) Mullins, O. C.; Sheu, E. Y. *Structure and Dynamics of Asphaltenes*; Plenum Press: New York, 1998.
- (18) McKenna, A. M.; Purcell, J. M.; Rodgers, R. P.; Marshall, A. G. *Energy Fuels* **2009**, *23*, 2122–2128.
- (19) Qian, K.; Mennito, A. S.; Edwards, K. E.; Ferrughelli, D. T. *Rapid Commun. Mass Spectrom.* **2008**, *22*, 2153–2160.
- (20) Dechaine, G.; Gray, M. *Energy Fuels* **2010**, *24*, 2795–2808.
- (21) Cosultchi, A.; Garciafigueroa, E.; Mar, B.; García-Bórquez, A.; Lara, V. H.; Bosch, P. *Fuel* **2002**, *81*, 413–421.
- (22) Hortal, A. R.; Hurtado, P.; Martínez-Haya, B.; Mullins, O. C. *Energy Fuels* **2007**, *21*, 2863–2868.
- (23) Gray, M.; Tykwiński, R.; Stryker, J.; Tan, X. *Energy Fuels* **2011**, *25*, 3125–3134.
- (24) Sheu, E. Y. *Energy Fuels* **2002**, *16*, 74–82.
- (25) Gawel, I.; Bociarska, D.; Biskupski, P. *Appl. Catal., A* **2005**, *295*, 89–94.
- (26) Wang, J.; Anthony, E. J. *Chem. Eng. Sci.* **2003**, *58*, 157–162.
- (27) Ancheyta, J.; Centeno, G.; Trejo, F.; Marroquin, G. *Energy Fuels* **2003**, *17*, 1233–1238.
- (28) Merdrignac, I.; Quoineaud, A.; Gauthier, T. *Energy Fuels* **2006**, *20*, 2028–2036.
- (29) Liu, D.; Li, Z.; Fu, Y.; Zhang, Y.; Gao, P.; Dai, C.; Zheng, K. *Energy Fuels* **2013**, *27*, 3692–3698.
- (30) Rueda-Velásquez, R. I.; Freund, H.; Qian, K.; Olmstead, W. N.; Gray, M. R. *Energy Fuels* **2013**, *27*, 1817–1829.
- (31) McKenna, A. M.; Marshall, A. G.; Rodgers, R. P. *Energy Fuels* **2013**, *27*, 1257–1267.
- (32) Chacón-Patiño, M. L.; Blanco-Tirado, C.; Orrego-Ruiz, J. A.; Gómez-Escudero, A.; Combariza, M. Y. *Energy Fuels* **2015**, *29*, 1323–1331.
- (33) Lababidi, S.; Panda, S. K.; Andersson, J. T.; Schrader, W. *Anal. Chem.* **2013**, *85*, 9478–9485.
- (34) ASTM Standard D6560-12, Standard test method for determination of asphaltenes (heptane insolubles) in crude petroleum and petroleum products. In *2012 Annual Book of ASTM Standards*; American Society for Testing and Materials (ASTM): West Conshohocken, PA, 2012.
- (35) Savage, P. E.; Klein, M. T.; Kukes, S. G. *Energy Fuels* **1988**, *2*, 619–628.
- (36) Karimi, A.; Qian, K.; Olmstead, W. N.; Freund, H.; Yung, C.; Gray, M. R. *Energy Fuels* **2011**, *25*, 3581–3589.
- (37) Kim, S.; Rodgers, R. P.; Marshall, A. G. *Int. J. Mass Spectrom.* **2006**, *251*, 260–265.
- (38) Stenson, A. C.; Marshall, A. G.; Cooper, W. T. *Anal. Chem.* **2003**, *75*, 1275–1284.
- (39) Siddiqui, M. N. *Fuel* **2003**, *82*, 1323–1329.
- (40) Gray, M.; Khorasheh, F.; Wanke, S.; Achia, U.; Krzywicki, A.; Sanford, E. C.; Sy, O. K. Y.; Ternan, M. *Energy Fuels* **1992**, *6*, 478–485.
- (41) Potapenko, O. V.; Doronin, V. P.; Sorokina, T. P.; Talsi, V. P.; Likhlobov, V. A. *Appl. Catal., B* **2012**, *117–118*, 177–184.
- (42) Jiménez Mateos, J. M.; Fierro, J. L. G. *Surf. Interface Anal.* **1996**, *24*, 223–236.
- (43) Islam, A.; Cho, Y.; Ahmed, A.; Kim, S. *Mass Spectrom. Lett.* **2012**, *3*, 63–67.
- (44) McKenna, A. M.; Blakney, G. T.; Xian, F.; Glaser, P. B.; Rodgers, R. P.; Marshall, A. G. *Energy Fuels* **2010**, *24*, 2939–2946.
- (45) Seki, H.; Kumata, F. *Energy Fuels* **2000**, *14*, 980–985.
- (46) Chiaberge, S.; Guglielmetti, G.; Montanari, L.; Salvalaggio, M.; Santolini, L.; Spera, S.; Cesti, P. *Energy Fuels* **2009**, *23*, 4486–4495.
- (47) Kawai, H.; Kumata, F. *Catal. Today* **1998**, *43*, 281–289.
- (48) Wiehe, I. A. In *Process Chemistry of Petroleum Macromolecules*; CRC Press: Boca Raton, FL, 2008; pp 97–179.
- (49) Schaub, T. M.; Rodgers, R. P.; Marshall, A. G.; Qian, K.; Green, L. A.; Olmstead, W. N. *Energy Fuels* **2005**, *19*, 1566–1573.
- (50) Purcell, J. M.; Rodgers, R. P.; Hendrickson, C. L.; Marshall, A. G. *J. Am. Soc. Mass Spectrom.* **2007**, *18*, 1265–1273.
- (51) Mullins, O. C. *Annu. Rev. Anal. Chem.* **2011**, *4*, 393–418.
- (52) Schucker, R. C.; Keweshan, C. F. In *Oil Shale, Tar Sands, and Related Materials*; American Chemical Society: Washington, DC, 2009; pp 327–346.
- (53) Strausz, O. P.; Mojelsky, T. W.; Faraji, F.; Lown, E. M.; Peng, P. *Energy Fuels* **1999**, *13*, 207–227.
- (54) Zhang, L.; Hou, Z.; Horton, S. R.; Klein, M. T.; Shi, Q.; Zhao, S.; Xu, C. *Energy Fuels* **2014**, *28*, 1736–1749.
- (55) Liu, P.; Xu, C.; Shi, Q.; Pan, N.; Zhang, Y.; Zhao, S.; Chung, K. H. *Anal. Chem.* **2010**, *82*, 6601–6606.
- (56) Lobodin, V. V.; Marshall, A. G.; Hsu, C. S. *Anal. Chem.* **2012**, *84*, 3410–3416.
- (57) Cho, Y.; Kim, Y. H.; Kim, S. *Anal. Chem.* **2011**, *83*, 6068–6073.
- (58) Hsu, C. S.; Lobodin, V. V.; Rodgers, R. P.; McKenna, A. M.; Marshall, A. G. *Energy Fuels* **2011**, *25*, 2174–2178.
- (59) Wu, Z.; Rodgers, R. P.; Marshall, A. G. *Anal. Chem.* **2004**, *76*, 2511–2516.
- (60) Kim, S.; Kramer, R. W.; Hatcher, P. G. *Anal. Chem.* **2003**, *75*, 5336–5344.
- (61) Podgorski, D. C.; Corilo, Y. E.; Nyadong, L.; Lobodin, V. V.; Bythell, B. J.; Robbins, W. K.; McKenna, A. M.; Marshall, A. G.; Rodgers, R. P. *Energy Fuels* **2013**, *27*, 1268–1276.
- (62) Speight, J. G. *Korean J. Chem. Eng.* **1998**, *15*, 1–8.
- (63) Savage, P. E.; Klein, M. T.; Kukes, S. G. *Ind. Eng. Chem. Process Des. Dev.* **1985**, *24*, 1169–1174.
- (64) Savage, P. E.; Klein, M. T. *Ind. Eng. Chem. Res.* **1988**, *27*, 1348–1356.
- (65) Strausz, O. P.; Mojelsky, T. W.; Lown, E. M. *Fuel* **1992**, *71*, 1355–1363.
- (66) Alshareef, A. H.; Scherer, A.; Tan, X.; Azyat, K.; Stryker, J. M.; Tykwiński, R. R.; Gray, M. R. *Energy Fuels* **2012**, *26*, 1828–1843.